

05,12,13

Planar ensembles of multilayer film microelements based on Cu/FeNi components

© G.Yu. Melnikov¹, V.N. Lepalovsky¹, A.V. Svalov¹, P. Lazpita²,
N.A. Buznikov³, G.V. Kurlyandskaya^{1,2}

¹ Ural Federal University after the first President of Russia B.N. Yeltsin,
Yekaterinburg, Russia

² University of the Basque Country UPV/EHU, Department of Electricity and Electronics,
48940 Leioa, Spain

³ Scientific Research Institute of Natural Gases and Gas Technologies, Gazprom VNIIGAZ,
Razvilka, Moscow Region, Russia

E-mail: grisha2207@list.ru

Received April 29, 2022

Revised April 29, 2022

Accepted May 12, 2022

Planar ensembles of multilayer periodic square microelements of the type $[\text{Cu}(6\text{ nm})/\text{FeNi}(100\text{ nm})]_5$ were obtained by ion-plasma sputtering on glass substrates using mesh copper masks. The surface features of trace elements were analyzed using a stylus profilometer, optical and scanning electron microscopy. Static magnetic properties and features of the magnetic domain structure were studied using the magneto-optical Kerr effect. The resulting planar ensembles can be used as an integral part of the film elements of weak magnetic field detectors operating on the basis of magnetic impedance (MI) to increase the sensitivity of the MI response to an external magnetic field. Keywords: multilayer film structures, ensembles of trace elements, periodic structures, giant magnetoimpedance effect.

Keywords: multilayer film structures, ensembles of trace elements, periodic structures, giant magnetoimpedance effect.

DOI: 10.21883/PSS.2022.09.54159.10HH

1. Introduction

Magnetic film elements with a periodic structure attract special attention, both from a theoretical point of view and due to various applications, such as magnetic memory devices, magnone crystals, materials with magnetocaloric effect features, magnetic sensors etc. [1–4].

Magnetic impedance (MI) is one of the phenomena effectively used to create sensors for weak magnetic fields [5]. MI means changing the impedance of a ferromagnetic conductor in an external magnetic field when a high-frequency current flows through it [6]. Symmetric or asymmetric multilayer structures (for example, based on components Cu/FeNi, Ti/FeNi, Ag/FeNi, etc.) in the form of strips oriented along the short side of the film element are used [6–8].

In paper [9] it was theoretically predicted that the creation of asymmetric MI film structures in the form of a traditional multilayer configuration $[\text{Cu}(6\text{ nm})/\text{FeNi}(100\text{ nm})]_5/\text{Cu}(500\text{ nm})$ and the ensemble of multilayer film microelements with a periodic structure as the upper magnetic layer above the copper central layer will increase the sensitivity of MI (it means changing the modulus of the MI ratio without taking into account the phase shift) with respect to the external magnetic field. At the same time, as the upper magnetic layer it was proposed to use the ensemble of multilayer film microelements with

the same periodic structure as the structure of the lower layer with the orientation of rectangular microelements along the short side of the main MI structure. Additionally, note that the periodic structure of the upper layer increases the effective surface area of the element, which is of great importance for the implementation of the surface functionalization process in the field of magnetic biodetection [9]. Thus, the search for the optimal periodic structure of the upper magnetic layer of MI elements and the creation of a stable technology for obtaining such structures is an important task.

In the present paper a method was proposed for obtaining ensembles of square multilayer film microelements with a periodic structure based on Cu/FeNi components, examples of such materials were obtained, and the features of their geometry, structure, and magnetic properties, including features of the domain structure were studied.

2. Measurement techniques and samples

Ensembles of square multilayer film microelements were obtained on glass substrates Corning 0.2 mm thick by the method of ion-plasma sputtering of a fused target with the composition $\text{Fe}_{20}\text{Ni}_{80}$. The following working parameters were used: initial pressure in the chamber $1.0 \cdot 10^{-7}$ mbar, argon working pressure $3.8 \cdot 10^{-3}$ mbar,

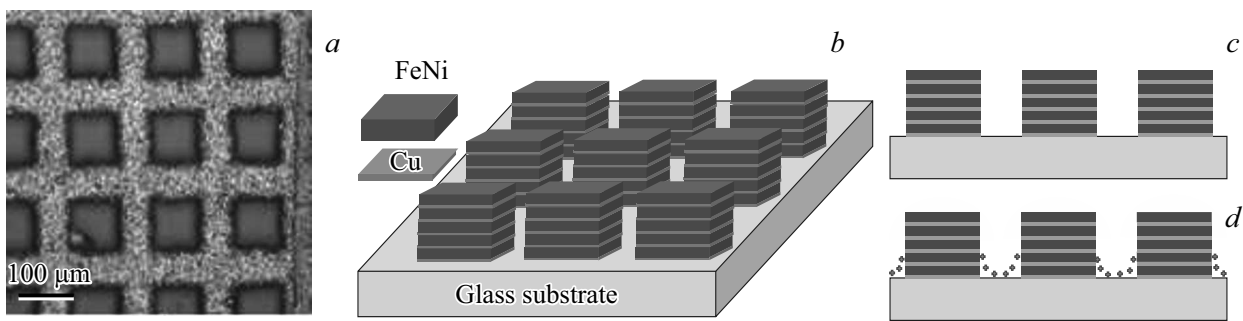


Figure 1. Photo of the grid for electron microscopy used as a mask for obtaining planar ensembles of multilayer film microelements (optical microscopy) (a); schematic representation of an ideal planar ensemble of multilayer film microelements MPFA (b) — side view and (c) — frontal projection; schematic representation of actual planar ensemble of multilayer film microelements MPFB (d).

technological magnetic field with the strength of 250 Oe was applied in the samples plane during their preparation to create induced uniaxial magnetic anisotropy.

Film samples of three types (total area of each type minimum $(7 \times 7 \text{ mm})$) were obtained and studied. The reference samples were a continuous multilayer film structure $[\text{Cu}(6 \text{ nm})/\text{FeNi}(100 \text{ nm})]_5$; this type of samples will be further referred to as MF. Ensembles of square multilayer film elements $[\text{Cu}(6 \text{ nm})/\text{FeNi}(100 \text{ nm})]_5$ were deposited on substrates using a copper grid for electron microscopy as a mask (square cell size was about $70 \mu\text{m}$, and the distance between them — about $30 \mu\text{m}$ (Fig. 1, a)). An external technological magnetic field was applied along one of the sides of the copper grid. Fixing the copper grid at different distances between the mask and the substrate made it possible to obtain ensembles of various types. Ensembles of microelements, mostly not in contact with each other, will be further referred to as MPFA, ensembles of microelements, most of which were in contact with each other at the base (on the surface of the substrate) — as MPFB. Fig. 1, b–c shows a schematic image of an ideal planar ensemble of MPFA multilayer film microelements, as well as a diagram of actual planar ensemble of microelements with the indication of zones of possible geometry deviations: shape rounding near sharp corners, possible material deposition in shaded areas. Besides, some thickness decreasing of all layers of the multilayer structure is possible.

The structural features were studied by X-ray phase analysis using a Philips X'pert PRO automatic diffractometer (operating parameters 40 kV and 40 mA) in theta-2theta configuration using a secondary monochromator and radiation $\text{Cu}-K_\alpha$ (the wavelength was $\lambda = 1.5418 \text{ \AA}$).

The magnetic properties (local magnetic hysteresis loops, i.e., the magnetization versus the magnitude of the applied external magnetic field $M(H)$, and the features of the magnetic domain structure) were studied using an Evico magnetics GmbH magneto-optical Kerr microscope at room temperature. temperature in the range of the external magnetic field from -100 Oe to 100 Oe .

3. Results and discussion

3.1. Features of the geometry of the surface layer and structure

Fig. 2 shows the results of structural studies of the obtained samples. The analysis of the average size microelements using optical and electron microscopy showed that the size of MPFA elements is close to $70 \pm 10 \mu\text{m}$, i.e., to the size of the mask slits. In the case of MPFB elements, the average size exceeds $100 \mu\text{m}$. At the same time, we faced great difficulties in determining the exact geometry of the lateral sides of the elements, because at a height of about 500 nm and close proximity of neighboring elements, problems both with the depth of focus of the image, and with the scattering of light and electron beam by the neighboring elements occur. Nevertheless, one can clearly see (Fig. 2, a–b), that ensembles of microelements close to the square shape with rounded corners are formed.

The profilometry data also confirm the fact that it was actually possible to obtain two types of ensembles of spatially separated microelements and microelements in contact with each other at the base. Although, according to the profilometry data, the height of individual microelements varied in the range from 100 to 300 nm depending on the distance between the mask and the substrate, the data on the total thickness of each element of the ensemble should be considered a qualitative assessment, since the resolution in this geometry is limited, and the error in determining the peak height can be up to 100 nm. However, the conclusion, that the total thickness of the microelement when deposited through the mask is less than the thickness of the reference multilayer structure, meets the expectation.

The X-ray spectra of the continuous MF structure contain a FeNi peak (111), which corresponds to the FCC lattice. The calculation according to Scherrer formula [10] makes it possible to estimate the average crystallite size, which was $15 \pm 3 \text{ nm}$. However, Cu peaks could not be observed in the spectrum, because the thickness of the interlayers is very small (6 nm), and, consequently, the total volume of

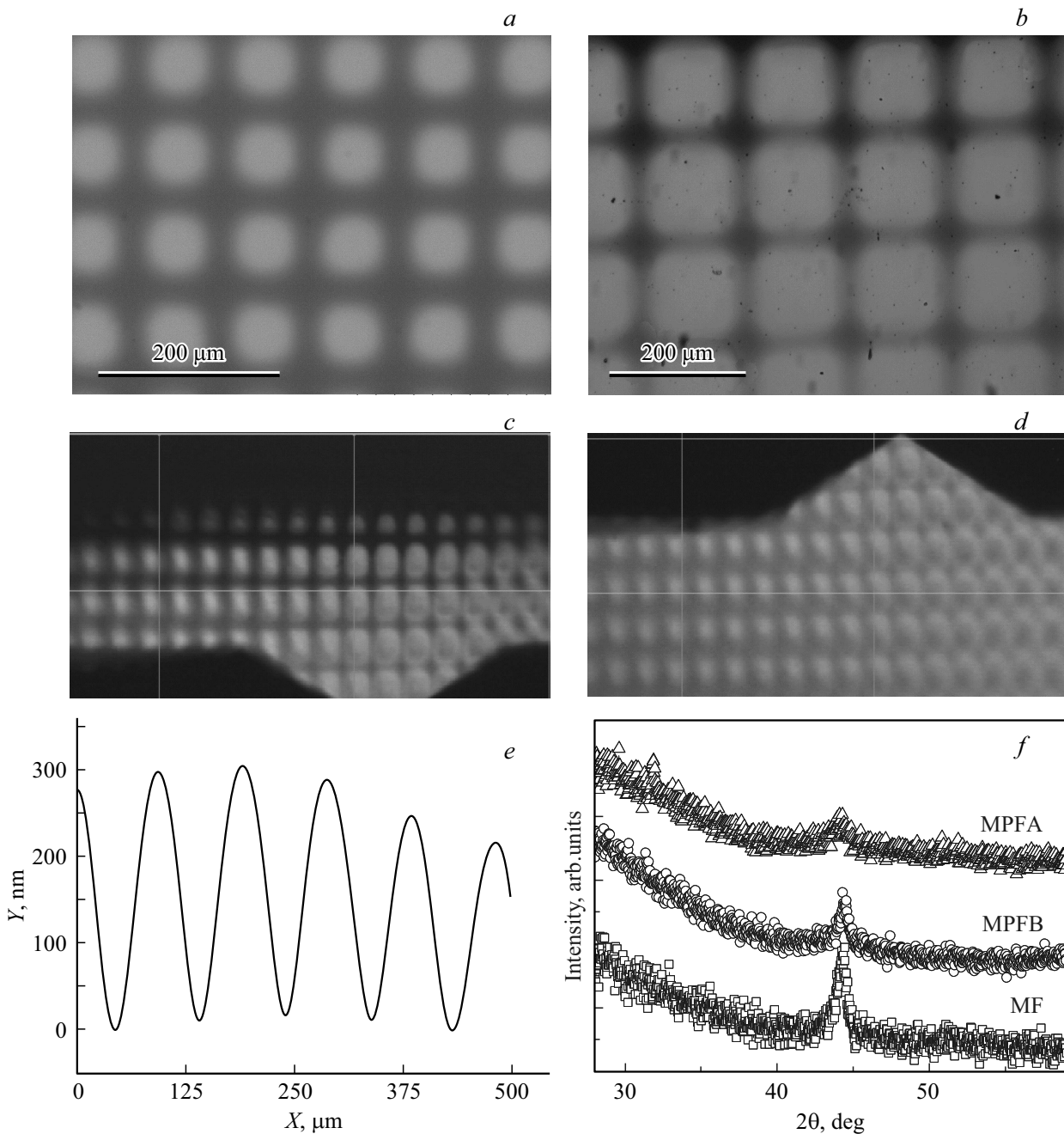


Figure 2. Features of the geometry of ensembles of periodic elements based on Cu/FeNi components: scanning electron microscopy, ensemble MPFB (a) optical microscopy, ensemble of the MPFA (b) type. An example of a stylus profilometer profile, an ensemble of the MPFA type (c) and MPFB (d–E). Results of an X-ray diffraction analysis of a continuous multilayer structure MF and ensembles of multilayer elements MPFA and MPFB (f).

the material involved in the XPA analysis is insufficient to obtain intense peaks.

The grain FeNi size in ensembles of periodic elements is somewhat smaller compared to FeNi in continuous film element and is about 8 ± 3 nm. This fact may indicate that the thickness of the FeNi layers in ensembles of elements is somewhat smaller, at least in the shading zones near the substrate. Additionally, we note that earlier, with a decrease in the thickness of FeNi, the fact of the grain

size decreasing at thicknesses close to 20 nm was observed repeatedly [11–13].

3.2. Magnetic properties

The reference sample in the form of a multilayer continuous MF structure based on Cu/FeNi components has a well-defined uniaxial effective magnetic anisotropy with the easy magnetization axis (EMA) oriented in the

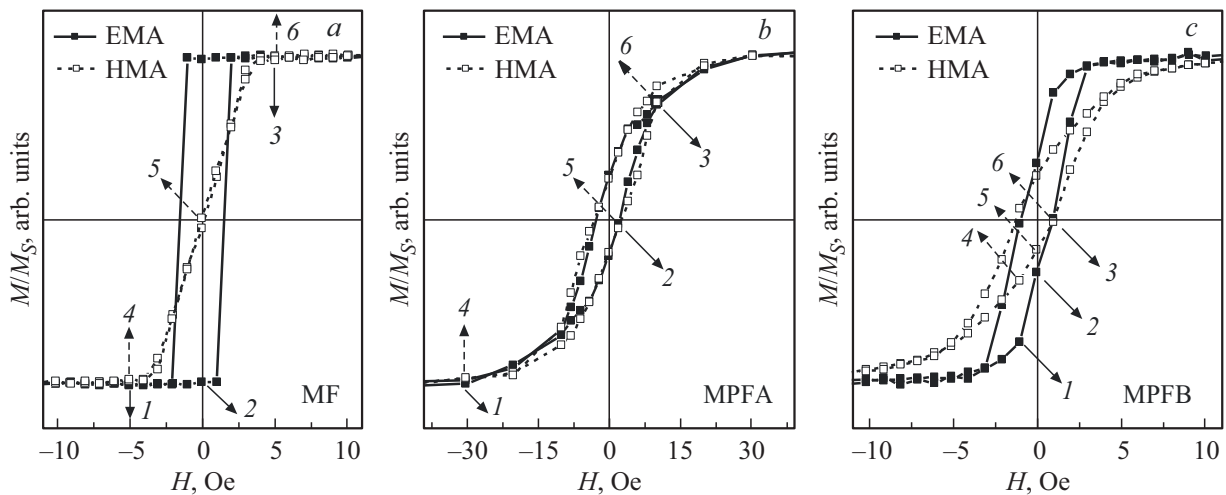


Figure 3. Magnetic hysteresis loops: (a) — multilayer continuous structure MF; (b) — multilayer periodic structure of separated MPFA elements; (c) — multilayer periodic structure of MPFB elements. The numbers mark the magnetic fields in which the photos of magnetic domains were obtained in Fig. 4, 5 and 6. EMA — easy magnetization axis, HMA — hard magnetization axis.

direction of the external technological field applied during sample preparation. The remagnetization along the EMA occurs due to the displacement of domain walls (Fig. 3, a), the coercive force (H_c) is about 1.5 Oe. In case of remagnetization along the hard magnetization axis (HMA), the process of remagnetization is close to the pure rotation of magnetic moments.

The processes of remagnetization of the MPFA sample (with a spatial separation of the ensemble microelements (Fig. 3, b) differ significantly from the processes of remagnetization of the multilayer structure MF. First, when the magnetic field is applied along the directions corresponding to the sides of the square elements the magnetic hysteresis loops become very close in all parameters — there is no magnetic anisotropy. Secondly, the shape of the hysteresis loop becomes more complicated, it becomes S-shaped, with a pronounced hysteresis ($H_c \approx 3$ Oe) and a magnetic saturation field above 30 Oe. With such a shape of the hysteresis loop, the remagnetization should be carried out in a complex manner involving both the rotation of magnetic moments and the displacement of domain boundaries.

The features of the effective magnetic anisotropy and the prevailing processes of remagnetization of the MPFB sample (without spatial separation of the ensemble microelements (Fig. 3, c) differ from both the MF case and MPFA case. The MPFB sample is characterized by the presence of effective magnetic anisotropy of the mixed type (magnetic hysteresis loops measured in the plane of the elements ensemble in the direction of the previously applied technological field and across it have different main characteristics). The magnitude of the coercive force in both cases is approximately 1.5 Oe. The shape of the magnetic hysteresis loop, measured in the direction of the previously applied process field, is slightly inclined, but rather rectangular at a fast saturation in a field of about 4 Oe. Remagnetization along this axis occurs mainly due to domain boundaries

displacement processes (Fig. 3, c). The shape of the magnetic hysteresis loop, measured in the perpendicular direction, approaches S-shaped one, but is characterized by a pronounced hysteresis and a magnetic saturation field above 10 Oe. With such a shape of the hysteresis loop, the processes of magnetic moments rotation should have a significant contribution, although both domain boundary displacements and irreversible rotation processes are quite probable (Fig. 3, c).

Fig. 4 shows the characteristic features of the magnetic domain structure of the ensemble of the MF type elements.

It is clearly seen that the magnetic structure is homogeneous. As expected, the remagnetization along the EMA proceeds by the displacement of the domain boundaries, and along the HMA — by the rotation of the spontaneous magnetization vectors.

Fig. 5 shows the characteristic features of the magnetic domain structure of the ensemble of the MPFA type elements.

It can be seen from photos of magnetic domains that the periodic geometry of the elements defines an ordered periodic magnetic structure with very similar domain features in each individual element, which is typical for all considered magnetic fields (Fig. 5). The boundaries between individual microelements are well defined both vertically and horizontally. The remagnetization along the EMA proceeds by shifting the domain boundaries oriented in the direction of the magnetic field. At the same time, in the regions at the edges where the normal component of the spontaneous magnetization vector breaks, apparently, a complex closure of the magnetic flux occurs with the formation of a magnetic structure of the vortex type. The remagnetization perpendicular to EMA has a complex nature and proceeds both through the magnetization rotation and through the displacement of the domain boundaries. However, in a zero field the circular

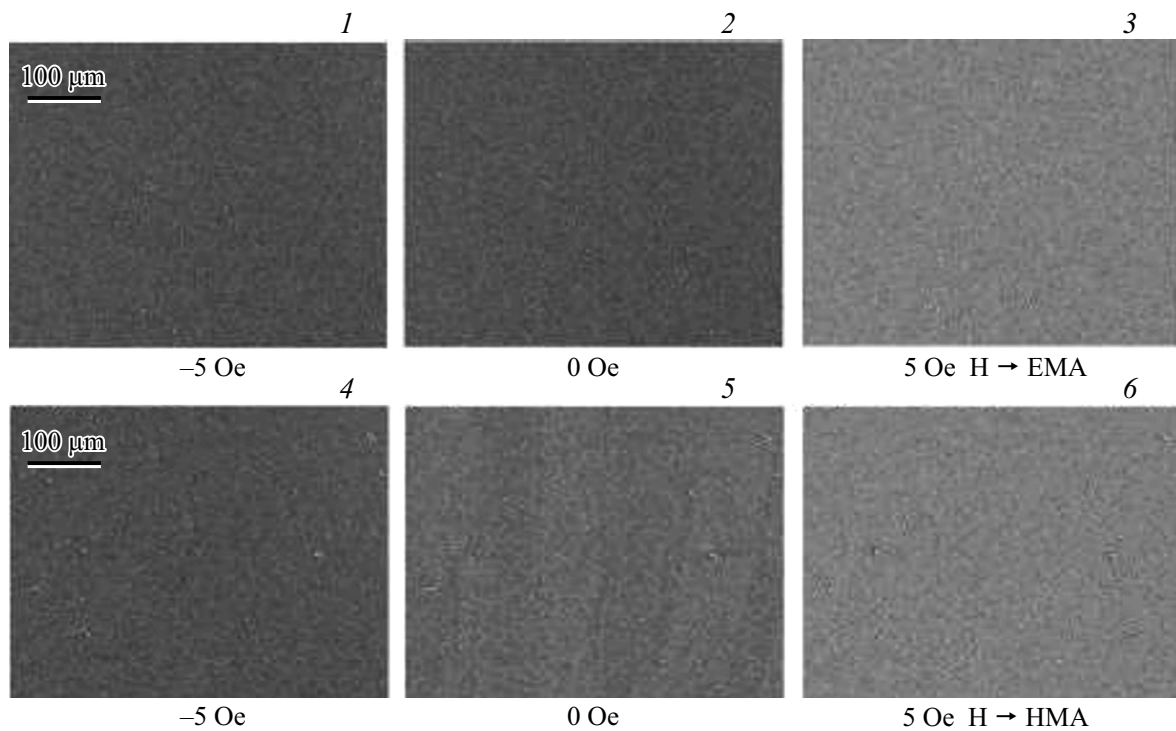


Figure 4. Magnetic domain structure of a continuous multilayer structure (MF). The outer fields marked with numbers (1–6), are chosen in accordance with the symbols in Fig. 3, *a*. EMA — easy magnetization axis, HMA — hard magnetization axis.

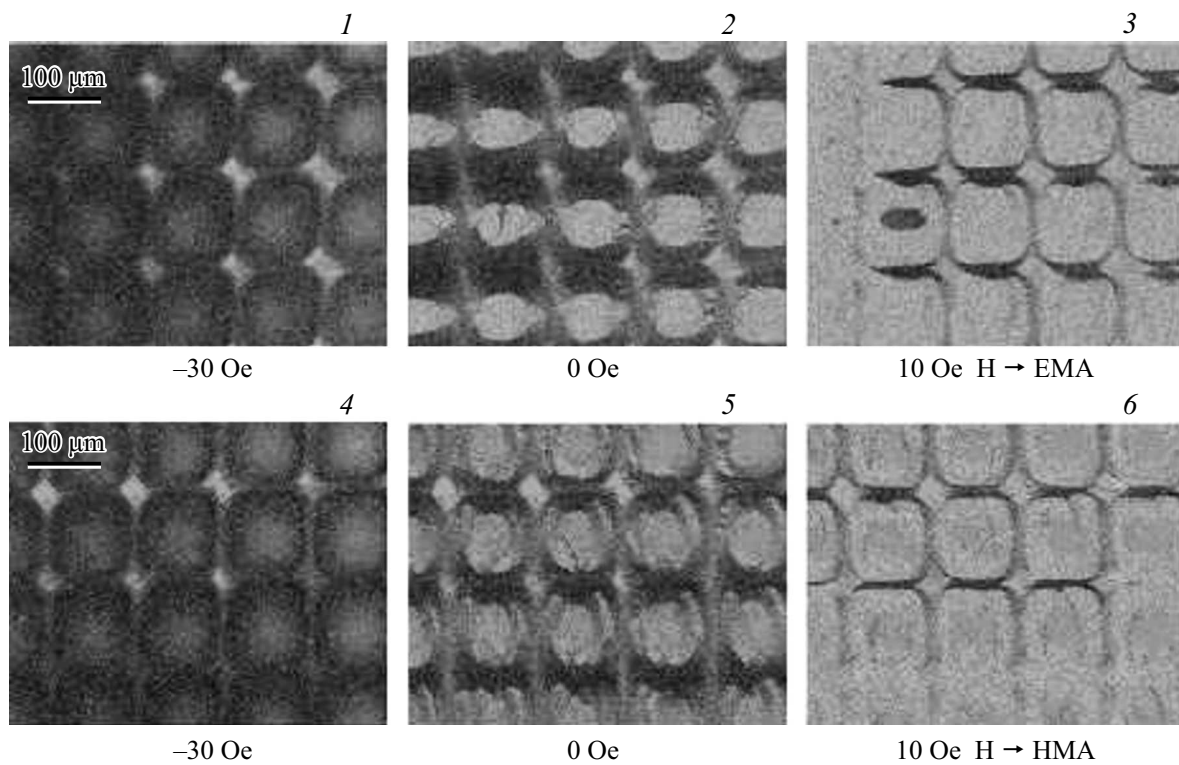


Figure 5. Magnetic domain structure of ensemble of periodic elements of the MPFA type. The outer fields marked with numbers (1–6), are chosen in accordance with the symbols in Fig. 3, *b*. EMA — easy magnetization axis, HMA — hard magnetization axis.

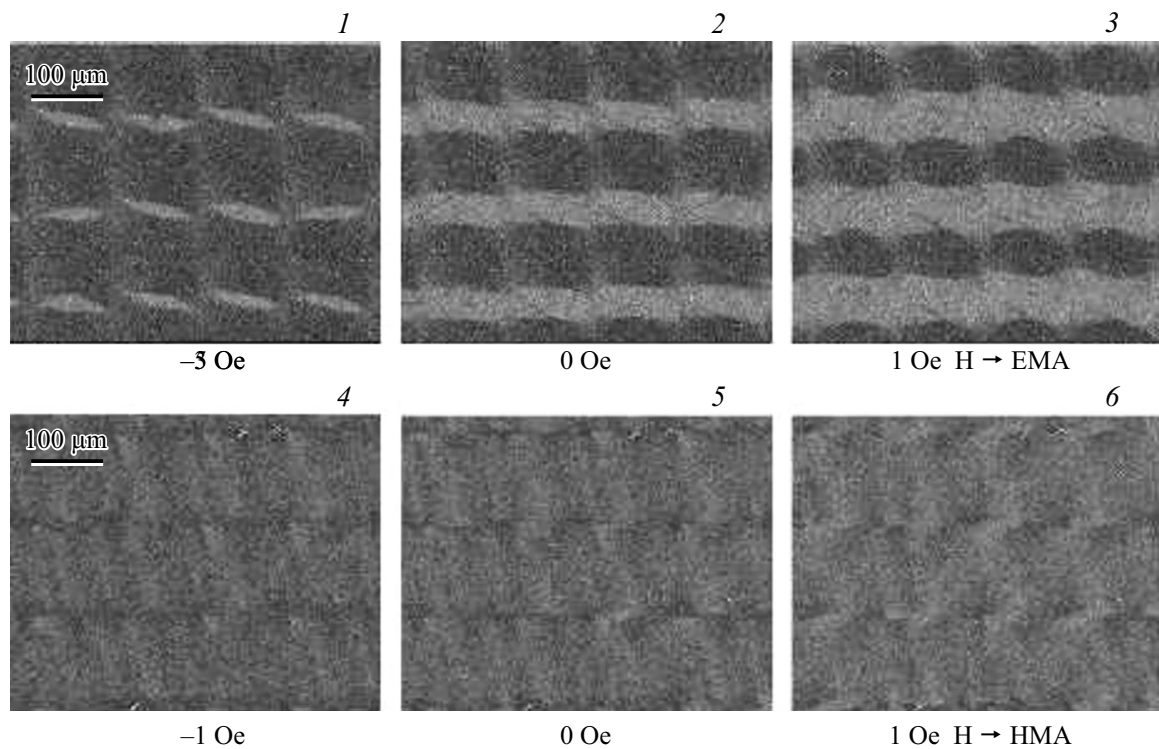


Figure 6. Magnetic domain structure of ensemble of periodic elements of the MPFB type. The outer fields marked with numbers (1–6), are chosen in accordance with the symbols in Fig. 3, c. EMA — easy magnetization axis, HMA — hard magnetization axis.

regions are reliably observed, where the magnetic anisotropy and shape anisotropy approximately compensate each other.

Fig. 6 shows the characteristic features of the magnetic domain structure of the ensemble of the MPFB type elements.

It can be seen from the photos of the domains that the external field application along the EMA sets an ordered periodic magnetic structure in the form of a vertical stripe structure with a width close to the width of the deposited elements. The boundaries between the columns of individual microelements show a magnetic structure with no noticeable features in the vertical regions between the deposited elements. However, neighboring microelements in each column, when remagnetized along the EMA, turn out to be separated by longitudinal domains, the length of which is close to the length of the elements, and the magnetization is oriented at a small angle to EMA. A further external field increasing along the EMA leads to the appearance of longitudinal domains, the length of which is close to the length of the elements, and the magnetization is oriented at a small angle to the EMA, but of the opposite sign. The external field application along the HMA defines the ordered periodic magnetic structure in the form of horizontal stripes with the width close to the height of the deposited elements. Remagnetization occurs by rotating the spontaneous magnetization vectors.

Note that for a more complete understanding of the remagnetization processes of the obtained 3D magnetic textures, additional studies are needed, including those

involving micromagnetic modeling. As noted earlier, the use of an ensemble of multilayer film microelements with the same periodic structure as the structure of the lower layer with the rectangular microelements orientation along the short side of the main MI structure can be of great importance for applications in the field of magnetic biodection [9]. Besides, obtaining 3D magnetic microtextures of various types [14–15] was of particular interest in recent years.

4. Conclusion

In the present paper the structure and magnetic properties of ensembles of multilayer films of the $[\text{Cu}(6 \text{ nm})/\text{FeNi}(100 \text{ nm})]_5$ type and ensembles of multilayer periodic square microelements based on them were obtained and studied. Depending on the distance between the mask and the substrate the structures of different types were obtained: an ensemble of square elements separated from each other or an ensemble of square elements, the lower parts of the faces of which merge in the shading zones. The periodic structures of microelement ensembles define ordered magnetic structures, the features of remagnetization of which were comparatively analyzed.

Funding

This work was financially supported by the Ministry of Science and Higher Education of the Russian Federation,

project No. FEUZ 2020-0051. This work was partially supported by funding from the GMMM Research Group of the University of the Basque Country. Separate studies were carried out in SPEAKER services UPV-EHU. The authors thank Dr. Ayton Larranaga for special support.

Conflict of interest

The authors declare that they have no conflict of interest.

References

- [1] T. Shinjo, T. Okuno, R. Hassdorf, K. Shigeto, T. Ono. *Science* **289**, 5481, 930 (2000).
- [2] J.A. Johnson, M. Grimsditch. *Appl. Phys. Lett.* **77**, 26, 4410 (2000).
- [3] D. Doblás, L.M. Moreno-Ramírez, V. Franco, A. Conde, A.V. Svalov, G. V. Kurlyandskaya. *Mater. Des.* **114**, 214 (2017).
- [4] S.A. Nikitov, D.V. Kalyabin, I.V. Lisenkov, A.N. Slavin, Yu.N. Barabanenkov, S.A. Osokin, A.V. Sadovnikov, E.N. Beginin, M.A. Morozova, Yu.P. Sharaevsky, Yu.A. Filimonov, Yu.V. Khivintsev, S.L. Vysotsky, V.K. Sakharov, E.S. Pavlov. *UFN*, **185** (1099) (2015) (in Russian).
- [5] N.A. Buznikov, A.P. Safronov, I. Orue, E.V. Golubeva, V.N. Lepalovskij, A.V. Svalov, A.A. Chlenova, G.V. Kurlyandskaya. *Biosens. Bioelectron.* **117**, 366 (2018).
- [6] N.A. Buznikov, A.V. Svalov, G.V. Kurlyandskaya. N.A. Buznikov, A.V. Svalov, G.V. Kurlyandskaya. *Phys. Met. Metallogr.* **122**, 223 (2021).]
- [7] M.A. Corrêa, F. Bohn, C. Chesman, R.B. da Silva, A.D.C. Viegas, R.L. Sommer. *J. Phys. D* **43**, 295004 (2010).
- [8] V.O. Vaskovsky, P.A. Savin, S.O. Volchkov, V.N. Lepalovsky, D.A. Bukreev, A.A. Buchkevich. *ZhTF* **83**, 1, 110 (2013) (in Russian).
- [9] N.A. Buznikov, G.V. Kurlyandskaya. N.A. Buznikov, G.V. Kurlyandskaya, *Phys. Met. Metallogr.* **122**, 8, 755 (2021).
- [10] M.L. Lobanov, A.S. Yurovskikh, N.I. Kardonina, G.M. Rusakov. *Metody issledovaniya tekstur v materialakh. Izd-vo Uralskogo un-ta, Ekaterinburg* (2014). 115 s. (in Russian).
- [11] M.A. Akhter, D.J. Mapps, Y.Q. Ma Tan. *J. Appl. Phys.* **81**, 8, 4122 (1997).
- [12] N.V. Alzola, G.V. Kurlyandskaya, A. Larranaga, A.V. Svalov. *IEEE Transact. Magn.* **48**, 4, 1605 (2012).
- [13] R. López Antón, J.A. González, J.P. Andrés, A.V. Svalov, G.V. Kurlyandskaya. *Nanomater.* **8**, 10, 780 (2018).
- [14] C. Donnelly, M. Guizar-Sicairos, V. Scagnoli, S. Gliga, M. Holler, J. Raabe, L.J. Heyderman. *Nature* **547**, 7663, 328 (2017).
- [15] A. Fernández-Pacheco, R. Streubel, O. Fruchart, R. Hertel, P. Fischer, R.P. Cowburn. *Nature Commun.*, **8**, 15756 (2017).